# A direct measurement of $|V\_cs|$ in hadronic W decays using a charm tag

R. Barate, D. Decamp, P. Ghez, C. Goy, S. Jezequel, J P. Lees, F. Martin, E. Merle, M N. Minard, B. Pietrzyk, et al.

LABORATOIRE EUROPEEN POUR LA PHYSIQUE DES PARTICULES (CERN)

CERN-EP/99-124
8 September 1999

# A direct measurement of $|V_{cs}|$ in hadronic W decays using a charm tag

ALEPH Collaboration [1]

**Abstract**

The inclusive charm production rate in W decays is measured from a study of the properties of final state particles. The sample of W pairs is selected from 67.7 $pb^{-1}$ collected by ALEPH in 1996 and 1997 at centre-of-mass energies near 172 and 183 GeV in the channels $W^+W^- \to 4q$ and $W^+W^- \to \ell\nu q\bar{q}$ . The branching fraction of hadronic W decays to a final state containing a c quark, $R_c^W = \Gamma(W \to cX)/\Gamma(W \to \text{hadrons})$, is measured to be $0.51 \pm 0.05_{\text{stat}} \pm 0.03_{\text{syst}}$. This allows a direct determination of the CKM matrix element $|V_{cs}| = 1.00 \pm 0.11_{\text{stat}} \pm 0.07_{\text{syst}}$.

(*Submitted to Physics Letters* **B**)

[1] See next pages for the list of authors

# The ALEPH Collaboration

R. Barate, D. Decamp, P. Ghez, C. Goy, S. Jezequel, J.-P. Lees, F. Martin, E. Merle, M.-N. Minard, B. Pietrzyk

*Laboratoire de Physique des Particules (LAPP), IN$^2$P$^3$-CNRS, F-74019 Annecy-le-Vieux Cedex, France*

R. Alemany, S. Bravo, M.P. Casado, M. Chmeissani, J.M. Crespo, E. Fernandez, M. Fernandez-Bosman, Ll. Garrido,[15] E. Graugès, A. Juste, M. Martinez, G. Merino, R. Miquel, Ll.M. Mir, P. Morawitz, A. Pacheco, I. Riu, H. Ruiz

*Institut de Física d'Altes Energies, Universitat Autònoma de Barcelona, 08193 Bellaterra (Barcelona), E-Spain*[7]

A. Colaleo, D. Creanza, M. de Palma, G. Iaselli, G. Maggi, M. Maggi, S. Nuzzo, A. Ranieri, G. Raso, F. Ruggieri, G. Selvaggi, L. Silvestris, P. Tempesta, A. Tricomi,[3] G. Zito

*Dipartimento di Fisica, INFN Sezione di Bari, I-70126 Bari, Italy*

X. Huang, J. Lin, Q. Ouyang, T. Wang, Y. Xie, R. Xu, S. Xue, J. Zhang, L. Zhang, W. Zhao

*Institute of High-Energy Physics, Academia Sinica, Beijing, The People's Republic of China*[8]

D. Abbaneo, U. Becker,[19] G. Boix,[6] O. Buchmüller, M. Cattaneo, F. Cerutti, V. Ciulli, G. Dissertori, H. Drevermann, R.W. Forty, M. Frank, F. Gianotti, T.C. Greening, A.W. Halley, J.B. Hansen, J. Harvey, P. Janot, B. Jost, I. Lehraus, O. Leroy, P. Maley, P. Mato, A. Minten, A. Moutoussi, F. Ranjard, L. Rolandi, D. Schlatter, M. Schmitt,[20] O. Schneider,[2] P. Spagnolo, W. Tejessy, F. Teubert, E. Tournefier, A.E. Wright

*European Laboratory for Particle Physics (CERN), CH-1211 Geneva 23, Switzerland*

Z. Ajaltouni, F. Badaud G. Chazelle, O. Deschamps, S. Dessagne, A. Falvard, C. Ferdi, P. Gay, C. Guicheney, P. Henrard, J. Jousset, B. Michel, S. Monteil, J-C. Montret, D. Pallin, P. Perret, F. Podlyski

*Laboratoire de Physique Corpusculaire, Université Blaise Pascal, IN$^2$P$^3$-CNRS, Clermont-Ferrand, F-63177 Aubière, France*

J.D. Hansen, J.R. Hansen, P.H. Hansen, B.S. Nilsson, B. Rensch, A. Wäänänen

*Niels Bohr Institute, 2100 Copenhagen, DK-Denmark*[9]

G. Daskalakis, A. Kyriakis, C. Markou, E. Simopoulou, A. Vayaki

*Nuclear Research Center Demokritos (NRCD), GR-15310 Attiki, Greece*

A. Blondel, J.-C. Brient, F. Machefert, A. Rougé, M. Swynghedauw, R. Tanaka, A. Valassi,[23] H. Videau

*Laboratoire de Physique Nucléaire et des Hautes Energies, Ecole Polytechnique, IN$^2$P$^3$-CNRS, F-91128 Palaiseau Cedex, France*

E. Focardi, G. Parrini, K. Zachariadou

*Dipartimento di Fisica, Università di Firenze, INFN Sezione di Firenze, I-50125 Firenze, Italy*

M. Corden, C. Georgiopoulos

*Supercomputer Computations Research Institute, Florida State University, Tallahassee, FL 32306-4052, USA* [13,14]

A. Antonelli, G. Bencivenni, G. Bologna,[4] F. Bossi, P. Campana, G. Capon, V. Chiarella, P. Laurelli, G. Mannocchi,[1,5] F. Murtas, G.P. Murtas, L. Passalacqua, M. Pepe-Altarelli

*Laboratori Nazionali dell'INFN (LNF-INFN), I-00044 Frascati, Italy*

M. Chalmers, L. Curtis, J.G. Lynch, P. Negus, V. O'Shea, B. Raeven, C. Raine, D. Smith, P. Teixeira-Dias, A.S. Thompson, J.J. Ward

*Department of Physics and Astronomy, University of Glasgow, Glasgow G12 8QQ,United Kingdom*[10]

R. Cavanaugh, S. Dhamotharan, C. Geweniger,[1] P. Hanke, V. Hepp, E.E. Kluge, A. Putzer, K. Tittel, S. Werner,[19] M. Wunsch[19]

*Institut für Hochenergiephysik, Universität Heidelberg, D-69120 Heidelberg, Germany*[16]

R. Beuselinck, D.M. Binnie, W. Cameron, P.J. Dornan,[1] M. Girone, S. Goodsir, N. Marinelli, E.B. Martin, J. Nash, J. Nowell, H. Przysiezniak, A. Sciabà, J.K. Sedgbeer, E. Thomson, M.D. Williams

*Department of Physics, Imperial College, London SW7 2BZ, United Kingdom*[10]

V.M. Ghete, P. Girtler, E. Kneringer, D. Kuhn, G. Rudolph

*Institut für Experimentalphysik, Universität Innsbruck, A-6020 Innsbruck, Austria*[18]

C.K. Bowdery, P.G. Buck, G. Ellis, A.J. Finch, F. Foster, G. Hughes, R.W.L. Jones, N.A. Robertson, M. Smizanska, M.I. Williams

*Department of Physics, University of Lancaster, Lancaster LA1 4YB, United Kingdom*[10]

I. Giehl, F. Hölldorfer, K. Jakobs, K. Kleinknecht, M. Kröcker, A.-S. Müller, H.-A. Nürnberger, G. Quast, B. Renk, E. Rohne, H.-G. Sander, S. Schmeling, H. Wachsmuth C. Zeitnitz, T. Ziegler

*Institut für Physik, Universität Mainz, D-55099 Mainz, Germany*[16]

J.J. Aubert, A. Bonissent, J. Carr, P. Coyle, A. Ealet, D. Fouchez, A. Tilquin

*Centre de Physique des Particules, Faculté des Sciences de Luminy, IN$^2$P$^3$-CNRS, F-13288 Marseille, France*

M. Aleppo, M. Antonelli, S. Gilardoni, F. Ragusa

*Dipartimento di Fisica, Università di Milano e INFN Sezione di Milano, I-20133 Milano, Italy.*

V. Büscher, H. Dietl, G. Ganis, K. Hüttmann, G. Lütjens, C. Mannert, W. Männer, H.-G. Moser, S. Schael, R. Settles, H. Seywerd, H. Stenzel, W. Wiedenmann, G. Wolf

*Max-Planck-Institut für Physik, Werner-Heisenberg-Institut, D-80805 München, Germany*[16]

P. Azzurri, J. Boucrot, O. Callot, S. Chen, M. Davier, L. Duflot, J.-F. Grivaz, Ph. Heusse, A. Jacholkowska,[1] M. Kado, J. Lefrançois, L. Serin, J.-J. Veillet, I. Videau,[1] J.-B. de Vivie de Régie, D. Zerwas

*Laboratoire de l'Accélérateur Linéaire, Université de Paris-Sud, IN$^2$P$^3$-CNRS, F-91898 Orsay Cedex, France*

G. Bagliesi, T. Boccali, C. Bozzi,[12] G. Calderini, R. Dell'Orso, I. Ferrante, A. Giassi, A. Gregorio, F. Ligabue, P.S. Marrocchesi, A. Messineo, F. Palla, G. Rizzo, G. Sanguinetti, G. Sguazzoni, R. Tenchini, A. Venturi, P.G. Verdini

*Dipartimento di Fisica dell'Università, INFN Sezione di Pisa, e Scuola Normale Superiore, I-56010 Pisa, Italy*

G.A. Blair, J. Coles, G. Cowan, M.G. Green, D.E. Hutchcroft, L.T. Jones, T. Medcalf, J.A. Strong

*Department of Physics, Royal Holloway & Bedford New College, University of London, Surrey TW20 OEX, United Kingdom*[10]

D.R. Botterill, R.W. Clifft, T.R. Edgecock, P.R. Norton, J.C. Thompson, I.R. Tomalin

*Particle Physics Dept., Rutherford Appleton Laboratory, Chilton, Didcot, Oxon OX11 OQX, United Kingdom*[10]

B. Bloch-Devaux, P. Colas, B. Fabbro, G. Faïf, E. Lançon, M.-C. Lemaire, E. Locci, P. Perez, J. Rander, J.-F. Renardy, A. Rosowsky, P. Saeger, A. Trabelsi,[21] B. Tuchming, B. Vallage

*CEA, DAPNIA/Service de Physique des Particules, CE-Saclay, F-91191 Gif-sur-Yvette Cedex, France*[17]

S.N. Black, J.H. Dann, C. Loomis, H.Y. Kim, N. Konstantinidis, A.M. Litke, M.A. McNeil, G. Taylor

*Institute for Particle Physics, University of California at Santa Cruz, Santa Cruz, CA 95064, USA*[22]

C.N. Booth, S. Cartwright, F. Combley, P.N. Hodgson, M. Lehto, L.F. Thompson

*Department of Physics, University of Sheffield, Sheffield S3 7RH, United Kingdom*[10]

K. Affholderbach, A. Böhrer, S. Brandt, C. Grupen, J. Hess, A. Misiejuk, G. Prange, U. Sieler

*Fachbereich Physik, Universität Siegen, D-57068 Siegen, Germany*[16]

G. Giannini, B. Gobbo

*Dipartimento di Fisica, Università di Trieste e INFN Sezione di Trieste, I-34127 Trieste, Italy*

J. Putz, J. Rothberg, S. Wasserbaech, R.W. Williams

*Experimental Elementary Particle Physics, University of Washington, WA 98195 Seattle, U.S.A.*

S.R. Armstrong, P. Elmer, D.P.S. Ferguson, Y. Gao, S. González, O.J. Hayes, H. Hu, S. Jin, J. Kile, P.A. McNamara III, J. Nielsen, W. Orejudos, Y.B. Pan, Y. Saadi, I.J. Scott, J. Walsh, J.H. von Wimmersperg-Toeller, Sau Lan Wu, X. Wu, G. Zobernig

*Department of Physics, University of Wisconsin, Madison, WI 53706, USA*[11]

[1]Also at CERN, 1211 Geneva 23, Switzerland.

[2]Now at Université de Lausanne, 1015 Lausanne, Switzerland.

[3]Also at Centro Siciliano di Fisica Nucleare e Struttura della Materia, INFN Sezione di Catania, 95129 Catania, Italy.

[4]Also Istituto di Fisica Generale, Università di Torino, 10125 Torino, Italy.

[5]Also Istituto di Cosmo-Geofisica del C.N.R., Torino, Italy.

[6]Supported by the Commission of the European Communities, contract ERBFMBICT982894.

[7]Supported by CICYT, Spain.

[8]Supported by the National Science Foundation of China.

[9]Supported by the Danish Natural Science Research Council.

[10]Supported by the UK Particle Physics and Astronomy Research Council.

[11]Supported by the US Department of Energy, grant DE-FG0295-ER40896.

[12]Now at INFN Sezione di Ferrara, 44100 Ferrara, Italy.

[13]Supported by the US Department of Energy, contract DE-FG05-92ER40742.

[14]Supported by the US Department of Energy, contract DE-FC05-85ER250000.

[15]Permanent address: Universitat de Barcelona, 08208 Barcelona, Spain.

[16]Supported by the Bundesministerium für Bildung, Wissenschaft, Forschung und Technologie, Germany.

[17]Supported by the Direction des Sciences de la Matière, C.E.A.

[18]Supported by Fonds zur Förderung der wissenschaftlichen Forschung, Austria.

[19]Now at SAP AG, 69185 Walldorf, Germany

[20]Now at Harvard University, Cambridge, MA 02138, U.S.A.

[21]Now at Département de Physique, Faculté des Sciences de Tunis, 1060 Le Belvédère, Tunisia.

[22]Supported by the US Department of Energy, grant DE-FG03-92ER40689.

[23]Now at LAL, 91898 Orsay, France.

# 1 Introduction

The data collected by ALEPH in the years 1996 and 1997, at average centre-of-mass energies of 172 GeV and 183 GeV, respectively, are used to study the properties of hadronic W boson decays. The total luminosity collected in the two periods is 67.7 $\mathrm{pb}^{-1}$ of which 57.0 $\mathrm{pb}^{-1}$ was collected at the higher energy. The identification of charm jets in these decays leads to a direct measurement of the fraction $\mathrm{R_c^W} = \Gamma(\mathrm{W} \to \mathrm{cX})/\Gamma(\mathrm{W} \to \mathrm{hadrons})$, where X stands for $\bar{\mathrm{d}}$, $\bar{\mathrm{s}}$ or $\bar{\mathrm{b}}$. Unless explicitly stated, the charge-conjugate modes are always implied throughout this paper. Within the Standard Model, this branching ratio can be expressed as a function of the different Cabibbo-Kobayashi-Maskawa (CKM) matrix elements through the following relation:

$$\mathrm{R_c^W} = \frac{|\mathrm{V_{cd}}|^2 + |\mathrm{V_{cs}}|^2 + |\mathrm{V_{cb}}|^2}{|\mathrm{V_{ud}}|^2 + |\mathrm{V_{us}}|^2 + |\mathrm{V_{ub}}|^2 + |\mathrm{V_{cd}}|^2 + |\mathrm{V_{cs}}|^2 + |\mathrm{V_{cb}}|^2}. \quad (1)$$

Assuming the unitarity of the CKM matrix, $\mathrm{R_c^W}$ is expected to be equal to 0.5. Therefore, a measurement of $\mathrm{R_c^W}$ is a direct test of this assumption. Furthermore, equation (1) can be used to extract a value of the least well known CKM matrix element $|\mathrm{V_{cs}}|$ which is currently measured to be $1.01 \pm 0.18$ using $\mathrm{D} \to \mathrm{K}\ell\nu_\ell$ decays [1].

A charm jet tagger (called $\mathrm{NN_c}$ in the following) was developed to identify $\mathrm{W} \to \mathrm{cX}$ decays. This is based on a neural network with 12 variables as input and uses mainly information from charm lifetime, jet-shape properties, reconstruction of D mesons and lepton identification. The procedure of extracting $\mathrm{R_c^W}$ and $|\mathrm{V_{cs}}|$ from the $\mathrm{NN_c}$ output is described in this paper. Another analysis based on a Fisher Discriminant technique is also presented as a crosscheck of the method.

# 2 The ALEPH detector

The ALEPH detector [2] and its performance [3] are described in detail elsewhere. Only a brief account of the parts of the apparatus relevant for this analysis is given here. Charged particles are detected over the range $|\cos\theta| < 0.95$ by an inner drift chamber and a large time projection chamber (TPC), complemented by a silicon strip vertex detector (VDET) made of two layers each providing measurements in the $r\phi$ and $rz$ coordinates, with a resolution of 12 $\mu$m in $r\phi$ and 12 $\mu$m in $rz$, for tracks at normal incidence. The three tracking detectors are immersed in a magnetic field of 1.5 T and together provide a transverse momentum resolution of $\delta(p_T)/p_T = 6 \times 10^{-4} p_T \oplus 0.005$ ($p_T$ in GeV/$c$) for high momentum charged particles.

The impact parameter of the tracks of charged particles with momentum in excess of 10 GeV/$c$ and reconstructed with two VDET coordinates is measured by the tracking system with a precision of 35 $\mu$m with respect to an event-by-event interaction point. This resolution allows c jets produced in $\mathrm{W} \to \mathrm{cX}$ decays to be selected by exploiting the longer lifetime of c hadrons with respect to other hadrons, using an algorithm based upon the track impact parameter measurement described in [4].

In addition to its rôle as a tracking device, the TPC is employed to separate charged particle species using up to 338 measurements of their specific ionization, $dE/dx$. This allows electrons to be separated from pions by more than three standard deviations up to a momentum of 8 GeV/$c$.

The electromagnetic calorimeter which surrounds the tracking detectors inside the superconducting solenoid is used, together with the TPC, to identify electrons and photons from the characteristic longitudinal and transverse profiles of their associated showers [3]. It consists of 45 layers of lead interleaved with proportional wire chambers, and covers the angular region $|\cos\theta| < 0.98$. The relative energy resolution achieved for isolated electromagnetic showers is $0.18/\sqrt{E} + 0.009$ ($E$ in GeV).

Muons are identified by their penetration pattern in the hadron calorimeter, composed of the iron of the magnet return yoke interleaved with 23 layers of streamer tubes, and by two muon chambers, each made of two layers of streamer tubes surrounding the calorimeter.

The total visible energy is measured with the energy-flow reconstruction algorithm described in [3]. This algorithm provides a list of charged and neutral reconstructed objects, called *energy-flow particles*, from which jets are reconstructed.

# 3 Monte Carlo samples

The value of $\mathrm{R_c^W}$ is extracted by comparing the $\mathrm{NN_c}$ output distribution in the data to the corresponding Monte Carlo distribution, where generated events are processed through a full simulation of the ALEPH detector response and through the same reconstruction chain. The KORALW [5] event generator with the complete set of WW-like four-fermion diagrams was used to produce two samples of 200,000 WW events at centre-of-mass energies of 172 GeV and 183 GeV, generated with reference W masses $\mathrm{M_W^{ref}}$ of 80.25 GeV/$\mathrm{c^2}$ and 80.35 GeV/$\mathrm{c^2}$, respectively. Additional samples with W mass equal to $\mathrm{M_W^{ref}} \pm 0.25$ GeV/$\mathrm{c^2}$ were used for checking purposes. Gluon radiation and the hadronisation process were simulated with the JETSET [6] package while the HERWIG [7] package was used for systematic studies. The decay properties of the $\mathrm{D^+}$, $\mathrm{D^0}$, and $\mathrm{D_s^+}$ mesons and of the $\Lambda_\mathrm{c}^+$ baryons were modified inside JETSET to reproduce those given by the MARKIII Collaboration [8] and the Particle Data Group [1]. This includes the exclusive branching ratios, the inclusive production rates of $\pi^0$, $\mathrm{K^0}$, $\bar{\mathrm{K}}^0$, $\mathrm{K^\pm}$, p, and $\Lambda$ and the topological branching ratios. The $\mathrm{c} \to \ell$ spectrum was also corrected by reweighting the energy spectrum given by JETSET in the centre-of-mass system of the decaying c hadron so that it reproduces the combined DELCO [9] and MARKIII [10] data.

PYTHIA [6] was used to generate the background processes $\mathrm{e^+e^-} \to \mathrm{q\bar{q}}(\gamma)$, ZZ, Zee and $\mathrm{We}\nu_\mathrm{e}$, with integrated luminosities corresponding to at least 50 times that of the data. Events with a flavour content that could originate from WW production were removed from the ZZ sample to avoid double counting with the KORALW sample.

# 4 Event selection and charm tag

## 4.1 Event selection

The event selection was performed separately for the purely hadronic events, $\mathrm{W^+W^-} \to 4\mathrm{q}$, and for the semileptonic events, $\mathrm{W^+W^-} \to \ell\nu\mathrm{q\bar{q}}$ ($\ell = \mathrm{e}, \mu$).

For the semileptonic events $\mathrm{W^+W^-} \to \mathrm{e}\nu\mathrm{q\bar{q}}$ and $\mathrm{W^+W^-} \to \mu\nu\mathrm{q\bar{q}}$ , the neural network described in Ref. [11] is used for the selection. The signal efficiency is about 90% for a purity of 95%. The selected events are then forced into two jets using the DURHAM-P [12]

algorithm, the lepton being removed when doing the clusterisation. Events corresponding to $W^+W^- \to \tau\nu q\bar{q}$ decays which pass this leptonic selection are treated as signal events in the fit procedure.

In the fully hadronic channel, a neural network package is again used to select the events. A description of this selection algorithm and the variables it uses, as well as the distribution of the neural network output, is given in [13]. This gives a signal efficiency of 83% for a purity of 86%. The selected events are forced into four jets using DURHAM-P, and the pairing of the jets is done by minimizing the quantity $(M_{ij} - M_W^{ref})^2 + (M_{kl} - M_W^{ref})^2$, where the subscripts i, j, k, l refer to the four jets.

The expected number of events in the different channels are listed in Table 1 for the two years of data taking. It has been checked that the selection efficiencies are the same for hadronic W decays with and without a charm quark and therefore the event selection does not bias the fraction of charm jets in W decays.

Table 1: Expected number of events for the semileptonic and hadronic WW decays and for the main background sources. The expected number of events are given for the integrated luminosity of 10.65 $pb^{-1}$ and 57.01 $pb^{-1}$ obtained at centre-of-mass energies of 172 and 183 GeV, respectively.

| Selection | 4q | $\ell\nu_\ell qq$ | $\tau\nu_\tau qq$ | $q\bar{q}(\gamma)$ | ZZ | Zee | MC | data |
|---|---|---|---|---|---|---|---|---|
| Semileptonic 172 | 0. | 30.6 | 1.0 | 0.4 | 0.1 | 0.2 | 32.3 | 31 |
| Hadronic 172 | 45.4 | 0.2 | 0.1 | 6.3 | 0.8 | 0. | 52.8 | 54 |
| Semileptonic 183 | 0.1 | 245. | 7.6 | 8. | 1. | 5. | 266.7 | 261 |
| Hadronic 183 | 322. | 0.5 | 0.6 | 46. | 2. | 0.1 | 371.2 | 400 |

## 4.2 Charm jet tagging

The discrimination of c jets (signal) and uds jets (background) produced in hadronic W decays is based on the following properties:

1. The lifetime of c hadrons is of the order of 1 ps; therefore, their decay products have on average large impact parameters.

2. D and $D^*$ mesons produced in the hadronization process can be reconstructed through their decay products.

3. The semileptonic branching ratio for c hadrons is about 10% [14], leading to a high rate of high energy leptons in the jets.

4. As the c quark is heavier than uds quarks and is weakly decaying, the jet-shape properties will be different. In particular the multiplicity of the decay products will be larger for D mesons. Furthermore these decay products will have specific momentum p and transverse momentum $p_\perp$ distributions (with respect to the jet axis).

From the above properties, twelve discriminating variables $V_i$ were built for each jet. In the following, the numbers in parentheses give the weights of each variable in the neural network, as defined in Ref. [15].

The variables exploiting the lifetime of charmed hadrons are

- $V_1$ (0.12): the logarithm of the lifetime probability of a jet to be a uds-jet [4].
- $V_2$ (0.07): the equivalent of $V_1$ but calculated only for charged tracks with $\eta_{\rm jet} > 4.9$ [15], where $\eta_{\rm jet}$ is the pseudorapidity of the track with respect to its jet axis.
- $V_3$ (0.08): a lifetime variable defined as the difference between the $\chi^2$ when all charged tracks of the jet are assigned to the primary vertex, and the sum of the primary and secondary vertex $\chi^2$ values when some tracks are transferred from the primary to a secondary vertex candidate [16].

The decay properties of charmed mesons are used in

- $V_4$ (0.06): the energy of the most energetic fully reconstructed D meson in the jet normalized to the beam energy. The D mesons are reconstructed in the following channels: $D^0 \to K^-\pi^+$, $D^0 \to K^-\pi^+\pi^+\pi^-$ and $D^+ \to K^-\pi^+\pi^+$ [17].
- $V_5$ (0.06): the $p_\perp^2$ of the $\pi_{\rm soft}$ candidate in $D^*$ decays, defined as the charged track in the jet with an energy between 1 and 4 GeV, having the smallest $p_\perp$ with respect to the jet axis [18].

The leptons produced in semileptonic decays of charmed hadrons are considered in

- $V_6$ (0.07): the number of leptons (electrons or muons) in the jet with $p \geq 2.5$ GeV/c. The criteria used to define leptons are those used for b physics studies at LEP1 [19].

Finally the larger mass of the charm quark with respect to u, d and s quarks is taken into account by

- $V_7$ (0.05): the energy of the nucleated system around the leading track of the jet, built with an invariant mass cut at 2.1 GeV/$c^2$ [20].
- $V_8$ (0.15): the sum of the pseudorapidities, calculated with respect to the jet axis, of the tracks within 40° of the jet axis.
- $V_9$ (0.09): the track multiplicity in a 40° cone around the jet-axis.
- $V_{10}$ (0.10): the momentum of the leading track in the jet.
- $V_{11}$ (0.04): the sphericity calculated with the four most energetic tracks of the jet [21].
- $V_{12}$ (0.11): the sum of the energies of the four most energetic tracks of the jet.

These jet variables are then used as input of a feed forward neural network with one hidden layer of 10 neurons, and an output layer consisting of one output node giving the variable $NN_c$ used to discriminate between c jets from W decays (output close to +1) and uds jets (output close to −1). The neural network was trained separately at 172 GeV and 183 GeV, and for semileptonic and 4q WW events. The distribution of some of these jet variables can be seen in Fig. 1 for the 183 GeV data. Figure 2 shows a comparison between data and Monte Carlo for the four input variables presented in Fig. 1. The shapes

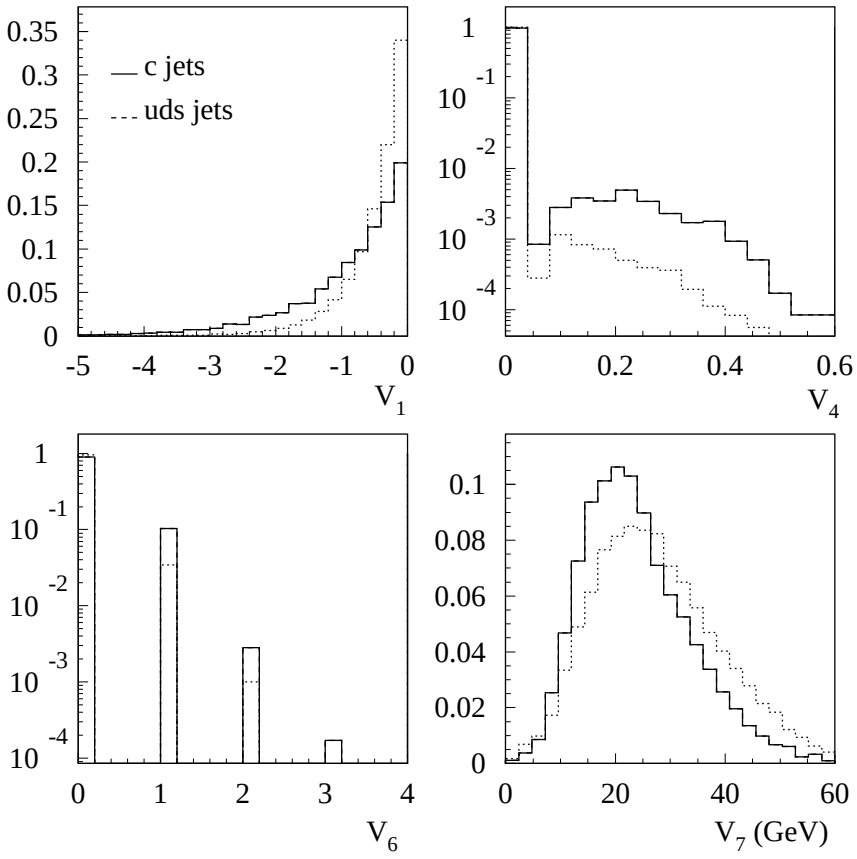


Figure 1: Distributions of four jet variables (among the twelve) used as input for $NN_c$ for c jets from W decays (signal) and uds jets from W decays (background) at 183 GeV. The two Monte Carlo contributions are normalized to the same number of entries. Similar distributions are obtained at 172 GeV. The contributions of $W^+W^- \to \ell\nu q\bar{q}$ and $W^+W^- \to 4q$ candidate events are added.

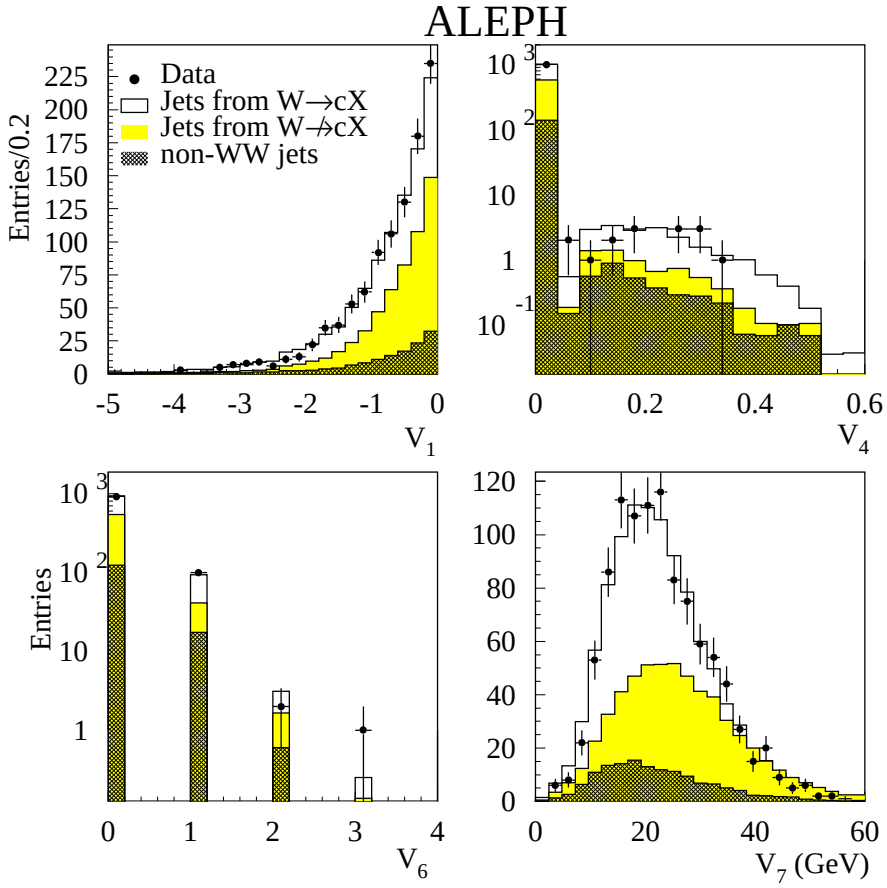


Figure 2: Distribution of four jet variables among the twelve used as input to $NN_c$. Comparison between data and Monte Carlo at 183 GeV for the most charm-like jet in the pair according to each variable. The contributions of $W^+W^- \to \ell\nu q\bar{q}$ and $W^+W^- \to 4q$ candidate events are added.

of the input variables and the performance of the neural network are very similar for the 172 GeV data.

The value of $NN_c$ is calculated for each of the jets of a pair, and the jet associated to the highest value, $NN_c^{max}$ , is chosen as the charm jet candidate and used in the analysis to determine $R_c^W$. The output distributions of $NN_c^{max}$ obtained for $W^+W^- \to \ell\nu q\bar{q}$ and $W^+W^- \to 4q$ events are shown in Fig. 3. The shapes of the two distributions are different because of possible overlapping of the jets in the $W^+W^- \to 4q$ channel. Figure 4 compares

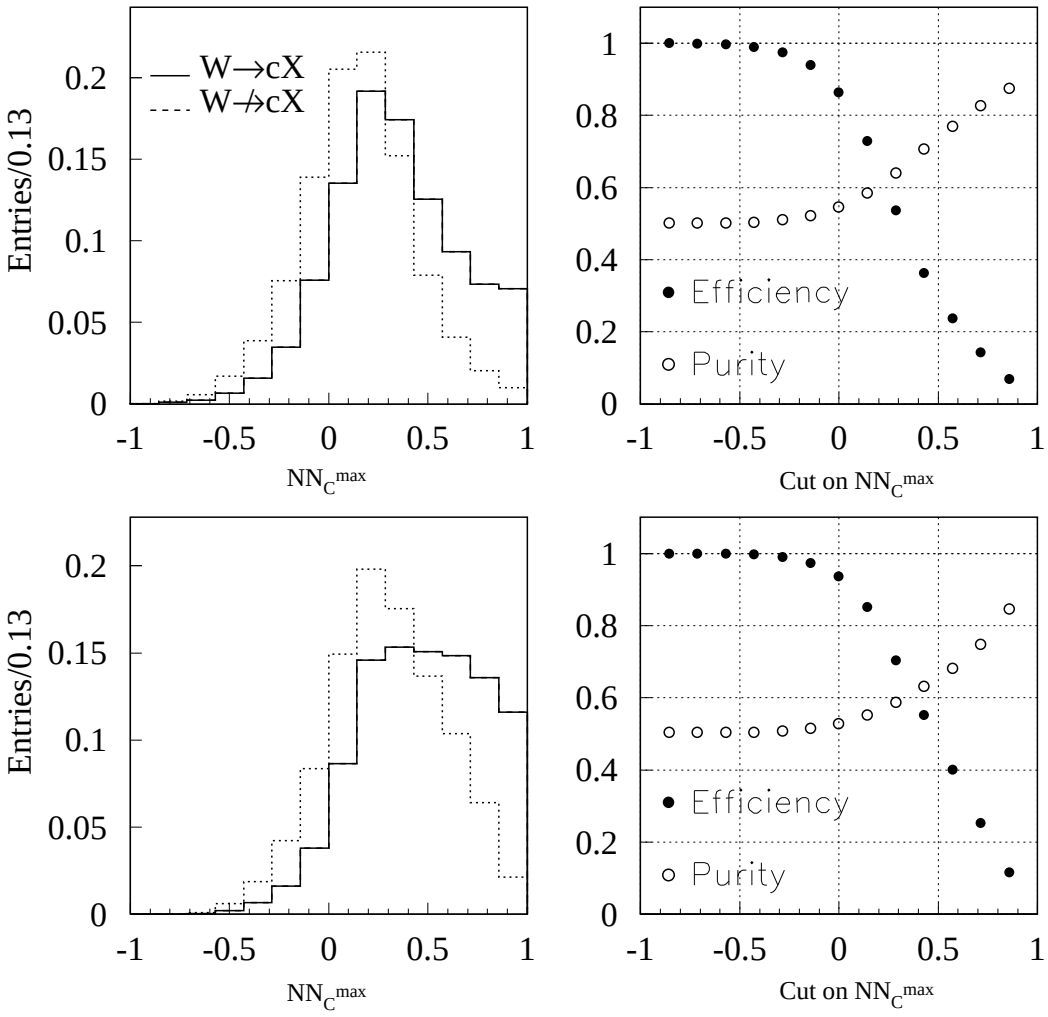


Figure 3: Monte Carlo output of $NN_c^{max}$ and its performance for the $W^+W^- \to \ell\nu q\bar{q}$ channel (upper plots) and the $W^+W^- \to 4q$ channel (lower plots). The purities are calculated using $R_c^W = 0.5$.

the distributions of $NN_c^{max}$ for data and Monte Carlo events. As there is one $W \to q\bar{q}'$ decay in semileptonic WW events, this channel contributes for one entry in Fig. 4. The two $W \to q\bar{q}'$ decays of a fully hadronic WW event contribute for two entries.

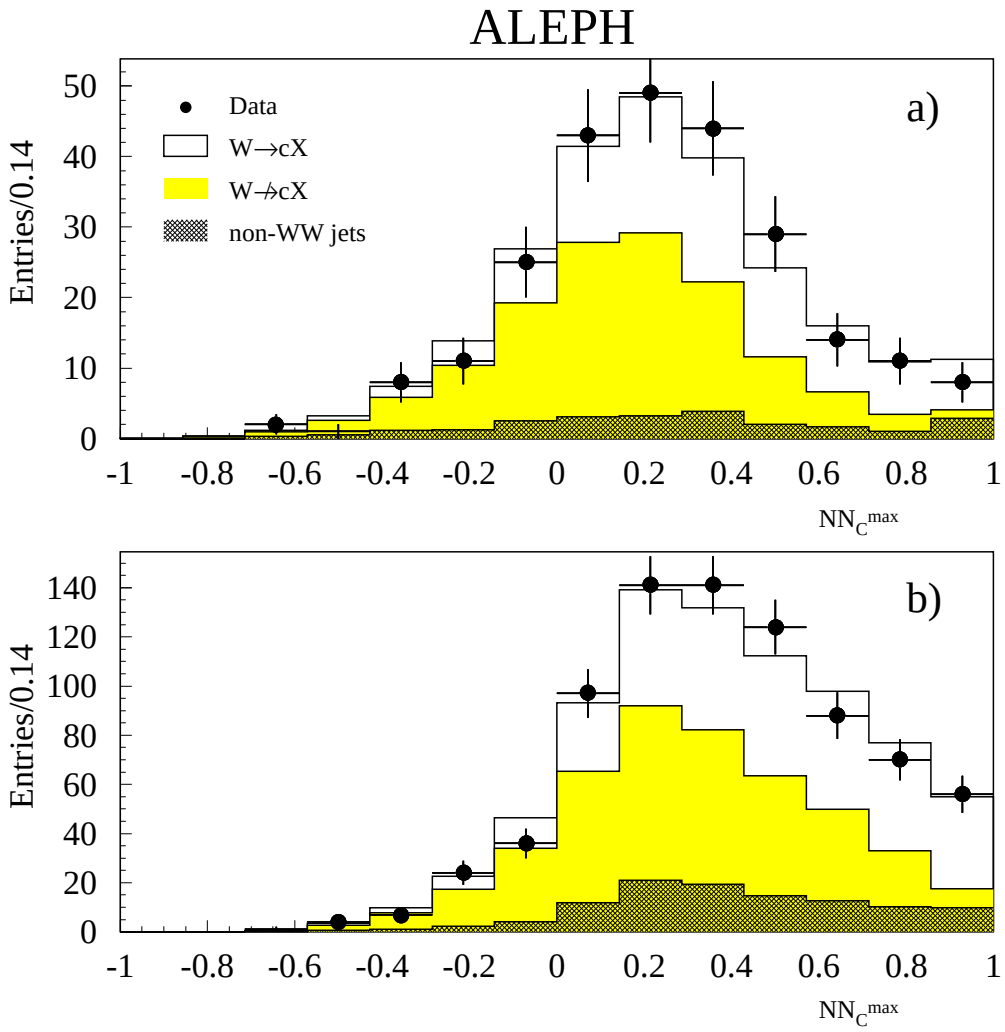


Figure 4: $NN_c^{max}$ output for the jet in the pair with the highest neural network output in a) $\ell\nu q\bar{q}'$ events and b) 4q events. Comparison between data and Monte Carlo normalized to the same number of entries.

# 5 Result

To extract $R_c^W$, a binned maximum likelihood fit is performed to the shape of the output distribution of $NN_c^{max}$. In each bin k of this distribution, the expected number of Monte Carlo events is defined as

$$\begin{aligned} N_k^{MC} &= R_c^W N_W Prob_{W\to cX}(k) + (1 - R_c^W) N_W Prob_{W\not\to cX}(k) \\ &\quad + N_{bkg} Prob_{bkg}(k) \end{aligned}$$

where $Prob_{W\to cX}(k)$, $Prob_{W\not\to cX}(k)$ and $Prob_{bkg}(k)$ are the probability density functions, determined from Monte Carlo, in the bin $k$ of the $NN_c^{max}$ distribution for the $W \to cX$, $W \not\to cX$ and non-WW background events, respectively. The total number $N_W$ of selected hadronic W decays is estimated as $N_{data} - N_{bkg}$, where $N_{data}$ and $N_{bkg}$ are respectively the total numbers of selected data and non-WW events; $N_{bkg}$ is estimated from Monte Carlo.

Setting $R_c^W$as free parameter in the fit, the result is $R_c^W = 0.57 \pm 0.18$ for the 172 GeV data and $R_c^W = 0.508 \pm 0.056$ for the 183 GeV data. The linearity of the fitted value of $R_c^W$ with the true input value is studied by generating seven different values of $R_c^W$ ranging from 20% to 80% in Monte Carlo samples treated as "data" and by fitting these samples with a reference Monte Carlo sample corresponding to $R_c^W = 0.50$. The relationship between the fitted value of $R_c^W$and the true value is found to be linear with a slope consistent with unity within a precision of 4% and no significant offset observed.

The expected statistical errors have been estimated as a check using a large number of Monte Carlo subsamples of the size of the data, and taking the mean value of the fit error distributions of these Monte Carlo subsamples for the expected errors. These are $\pm 0.16$ and $\pm 0.056$ for the 172 GeV and 183 GeV data, respectively, in agreement with the fit errors. Furthermore, the pulls of the fitted $R_c^W$values have RMS and means compatible with 1 and 0. Using the fit errors, the combined result is

$$R_c^W = 0.515 \pm 0.053.$$

The values obtained for the semileptonic and fully hadronic channels are $0.537 \pm 0.104$ and $0.505 \pm 0.063$, respectively.

From the world average values $|V_{ud}| = 0.9736 \pm 0.0010$, $|V_{us}| = 0.2205 \pm 0.0018$, $|V_{ub}| = 0.0033 \pm 0.0008$, $|V_{cd}| = 0.224 \pm 0.016$ and $|V_{cb}| = 0.041 \pm 0.003$ [1], the value of $|V_{cs}|$ derived from the measurement of $R_c^W$is $1.13^{+0.50}_{-0.33}$ with the 172 GeV data and $0.99^{+0.12}_{-0.11}$ with the 183 GeV data, leading to the result

$$|V_{cs}| = 1.00 \pm 0.11.$$

The values obtained for the semileptonic and hadronic channels are $1.05 \pm 0.24$ and $0.98 \pm 0.13$, respectively.

# 6 Studies of systematic uncertainties

The following sources of systematic errors are considered:

1. An uncertainty of 5% is applied to the normalization of the $q\bar{q}(\gamma)$ background as estimated in Ref. [22].

2. The error resulting from the particular choice of QCD Monte Carlo generator is estimated by replacing JETSET by HERWIG for both the $q\bar{q}(\gamma)$ background and the $W \to q\bar{q}$ decays, and the full difference between the two results is taken as the systematic error. Since HERWIG is known to provide a very approximate representation of exclusive properties of hadronisation, this estimate is very conservative.

3. The effect of color reconnection is estimated by using three samples of fully simulated HERWIG WW events generated with the $P_{\mathrm{RECO}}$ parameter, defining the level of reconnection probability, set to 0%, 11% and 60%, respectively [23]. The largest shift obtained relative to the 0% connected sample is taken as the systematic error.

4. Effects of possible calorimeter miscalibration are studied by varying the response of the electromagnetic and hadronic calorimeters by 0.9% and 2% respectively.

5. Standard track momentum corrections are applied to all tracks in WW events; the systematic error is assessed by comparing the result of the fit obtained with and without the corrections.

6. The distribution of the track impact parameter significance in Monte Carlo events was corrected by means of the procedure described in [4], so that data and Monte Carlo have the same resolution. The associated systematic error is estimated by taking the difference of the $R_c^W$ values obtained with and without this correction.

7. The mass of the W boson in the Monte Carlo is varied by $\pm 90$ MeV/$c^2$.

8. The JADE [24] algorithm is used to form the jets instead of DURHAM-P.

9. Since this analysis is based on the properties of the decay products of the charmed hadrons, the effects related to charm production (relative production rates of the $D^0$, $D^+$, $D_s^+$, and $\Lambda_c$), charm fragmentation and charm decay properties (D meson topological branching ratios, inclusive production of $K^0$, $\bar{K}^0$, $K^\pm$, and $\pi^0$) are studied in detail following the recommendations of [14].

The different sources of systematic uncertainties and the corresponding relative errors are summarized in Table 2.

# 7 Checks of the analysis

The consistency of the $NN_c^{max}$ distribution in data and Monte Carlo is tested by means of a Kolmogorov test. This gives a consistency confidence level of 98.1% if the fitted value of $R_c^W$is used in the simulation, while this confidence level becomes smaller than 1% if $R_c^W$is set to zero.

The number of fully reconstructed D mesons in the most charm-like jet of a pair is 21 in the data; 22.6 are expected in the simulation using the fitted value of $R_c^W$, while only 9.8 would be expected without $W \to cX$ transitions. The number of energetic lepton candidates observed in the data is 122, while 108.5 (72.1) are expected in the simulation with (without) $W \to cX$ transitions.

Table 2: Systematic errors on $R_c^W$.

| Source | $\Delta R_c^W$ $(10^{-2})$ |
|---|---|
| Background normalization | 0.2 |
| Hadronization | 2.9 |
| Color reconnection | 0.3 |
| Calorimeter calibration | 0.9 |
| Tracking error | 0.3 |
| Impact parameter resolution | 0.4 |
| Mass of the W boson | 0.4 |
| Jet algorithm | 0.4 |
| Charm production | 0.1 |
| Charm fragmentation | 0.3 |
| Charm decay properties | 0.9 |
| Total Error | 3.3 |

Figure 5 shows the variation of $R_c^W$as a function of a cut on the output of $NN_c^{max}$. Its value is seen to be stable within the variation allowed by the uncorrelated statistical errors.

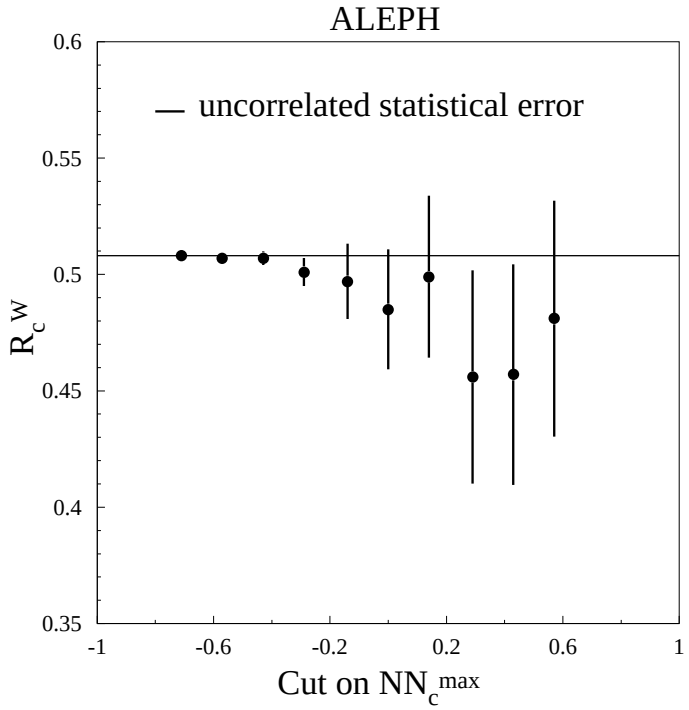


Figure 5: Values of the branching ratio $R_c^W$obtained at 183 GeV for different cuts on $NN_c^{max}$. The uncorrelated statistical errors are calculated with respect to a cut at $-0.6$, and the solid line shows the fitted value of $R_c^W$.

Finally, an alternative approach was developed as a check of the previous method. It is based on a Fisher Discriminant Analysis (FDA) [25] using dijets to tag the $W \to cX$ final

state. For this analysis, 12 variables closely related to those used in the neural net analysis were chosen to perform the discrimination. Each of these variables is calculated for each jet of a hadronic W decay, giving two values. The most charm-like value is then chosen and used as input to the FDA to form a single variable $Y_c$. This corresponds to a tag of W→cX decays and is different from the procedure used in the previous analysis which chooses between the two jets of a pair at the level of the $NN_c$ output. Figure 6 displays the FDA output for the hadronic W decays in the semileptonic and the hadronic WW events. The output distribution of $Y_c$ is fitted in the same way as in Section 5

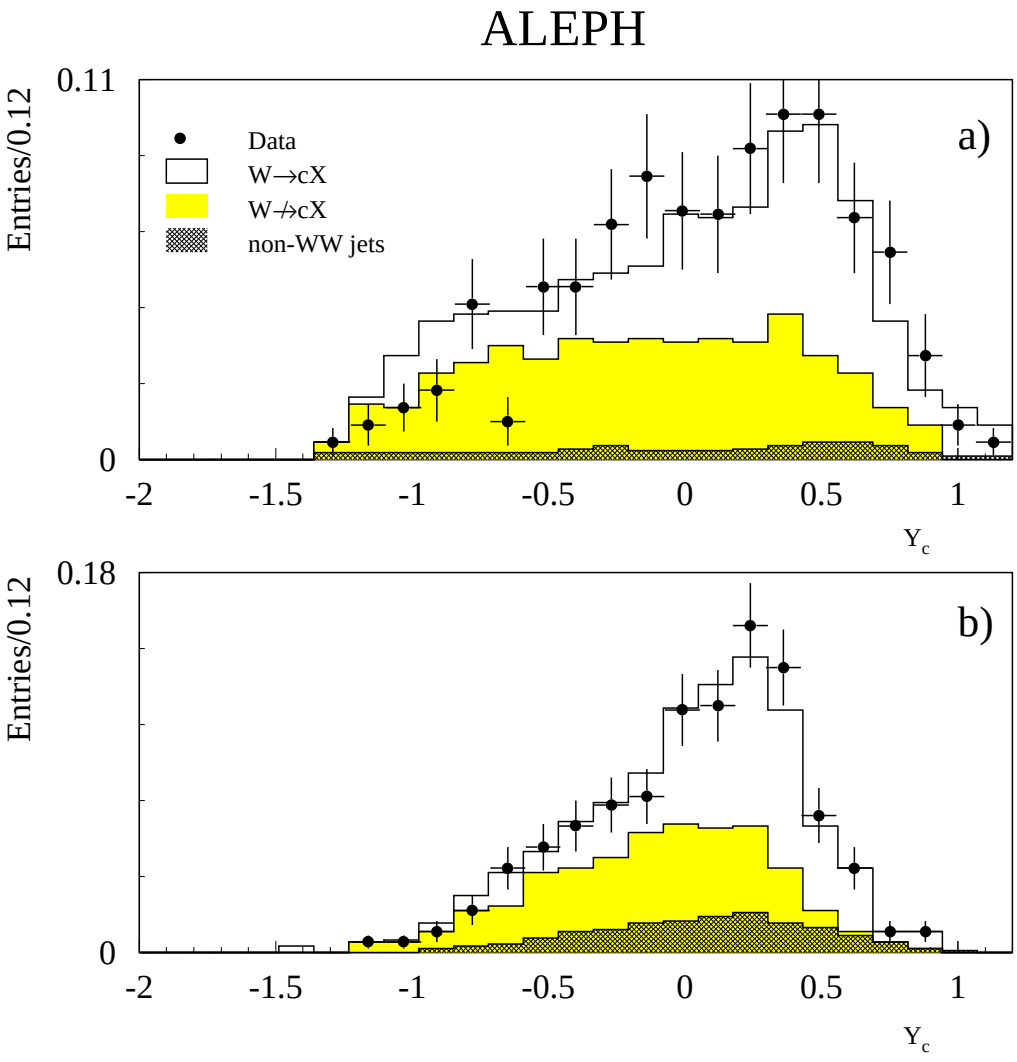


Figure 6: Distribution of the FDA output $Y_c$ for a) $W^+W^- \to \ell\nu q\bar{q}$ and b) $W^+W^- \to 4q$ events. Comparison between data and Monte Carlo.

to get a measurement of $R_c^W$and $|V_{cs}|$. The result of the fit, $R_c^W = 0.503 \pm 0.065$ and $|V_{cs}| = 0.973 \pm 0.138$, is in agreement with that from the neural network analysis, with a larger statistical uncertainty.

# 8 Conclusion

Using a charm tag based on the properties of jets produced in W decays, the inclusive charm production rate in W decays, $R_c^W$, is measured. The analysis of the 172−183 GeV data collected by ALEPH in 1996 and 1997 leads to the value

$$R_c^W = \Gamma(W \to cX)/\Gamma(W \to \text{hadrons}) = 0.51 \pm 0.05_{\text{stat}} \pm 0.03_{\text{syst}},$$

from which the value

$$|V_{cs}| = 1.00 \pm 0.11_{\text{stat}} \pm 0.07_{\text{syst}}$$

is derived. The measured value of $R_c^W$is in agreement with the Standard Model expectation of 0.5 assuming the unitarity of the CKM matrix and with the result obtained by the DELPHI collaboration [26].

This result can be combined with the indirect measurement, $|V_{cs}| = 1.043 \pm 0.058_{\text{stat}} \pm 0.026_{\text{syst}}$, obtained from the hadronic branching ratio measurement at 161, 172 and 183 GeV [27]. The statistical errors of the two analyses are assumed to be uncorrelated and the common systematic errors are taken to be fully correlated. The weights of the direct and indirect measurements in this average are 21% and 79%, respectively. This leads to the result

$$|V_{cs}|(\text{combined}) = 1.034 \pm 0.051_{\text{stat}} \pm 0.029_{\text{syst}}.$$

# Acknowledgment

We are indebted to our colleagues of the accelerator divisions for the outstanding performance of the LEP accelerator. Thanks are also due to the many engineering and technical personnel at CERN and at the home institutes for their contributions toward the success of ALEPH. Those of us not from member states wish to thank CERN for its hospitality.

# References

[1] Particle Data Group, *Review of Particle Physics*, Phys. Rev. **D54** (1996) 1.

[2] ALEPH Collaboration, *ALEPH: a detector for electron-positron annihilations at LEP*, Nucl. Inst. and Meth. **A294** (1990) 121.

[3] ALEPH Collaboration, *Performance of the ALEPH detector at LEP*, Nucl. Inst. and Meth. **A360** (1995) 481.

[4] ALEPH Collaboration, *A measurement of* $R_b$ *using a lifetime-mass tag.* Phys. Lett. **B401** (1997) 150.

[5] M. Skrzypek, S. Jadach, W. Placzek and Z. Wąs, Comp. Phys. Commun. **94** (1996) 216.

[6] T. Sjöstrand, Comp. Phys. Commun. **82** (1994) 74.

[7] G. Marchesini et al., Comp. Phys. Commun. **67** (1992) 465.

[8] MARKIII Collaboration, *Measurement of the inclusive decay properties of charmed mesons*, Phys. Lett. **B263** (1991) 135.

[9] DELCO Collaboration, *Semileptonic Decays on the D meson*, Phys. Rev. Lett. **43** (1979) 1073.

[10] MARKIII Collaboration, *Direct Measurement of charmed $D^+$ and $D^0$ Semileptonic Branching Ratios*, Phys. Rev. Lett. **54** (1985) 1976.

[11] ALEPH Collaboration, *Measurement of the Triple Gauge-Boson Couplings at 172 GeV*, Phys. Lett. **B422** (1998) 369.

[12] Yu. L. Dokshitzer, J. Phy **G17** (1991) 1441.

[13] ALEPH Collaboration, *Measurement of the W Mass by direct Reconstruction in e+e- Collisions at 172 GeV*, Phys. Lett. **B422** (1998) 384.

[14] The LEP experiments: ALEPH, DELPHI, L3 and OPAL, *Combining Heavy Flavour Electroweak Measurements at LEP*, Nucl. Inst. and Meth. **A378** (1996) 101.

[15] ALEPH Collaboration, *A measurement of* $\mathrm{R_b}$ *using mutually exclusive tags.* Phys. Lett. **B401** (1997) 163.

[16] ALEPH Collaboration, *An investigation of $B_d^0$ and $B_s^0$ oscillations*, Phys. Lett. **B322** (1994) 441.

[17] ALEPH Collaboration, *The forward-backward asymmetry for charm quarks at the Z pole*, Phys. Lett. **B352** (1995) 479.

[18] ALEPH Collaboration, *Measurement of the branching fraction for* $\mathrm{D^0 \to K^-\pi^+}$, CERN-PPE/97-024, submitted to Phys. Lett. B.

[19] ALEPH Collaboration, *Heavy flavour production and decay with prompt leptons in the ALEPH detector*, Z. Phys. **C62** (1994) 179.

[20] ALEPH Collaboration, *Measurements of mean lifetime and branching fractions of b hadrons decaying to $J/\psi$*, Phys. Lett. **B295** (1992) 396.

[21] L. Bellantoni et al., Nucl. Inst. and Meth. **A310** (1991) 618.

[22] ALEPH Collaboration, *Measurement of the W mass in* $\mathrm{e^+e^-}$ *collisions at production threshold*, Phys. Lett. **B401** (1997) 347.

[23] Working group on the W mass in "Physics at LEP2", CERN 96-01 (1996), Vol. 1, 190.

[24] JADE Collaboration, Z. Phys. **C33** (1986) 23; Phys. Lett. **B213** (1988) 235.

[25] R.A. Fisher, Ann. Eugen. **7** (1936) 179.

[26] DELPHI Collaboration, *Measurement of* $|\mathrm{V_{cs}}|$ *using W decays at LEP2*, Phys. Lett. **B439** (1998) 209.

[27] ALEPH Collaboration, *Measurement of W-pair production in* $\mathrm{e^+e^-}$ *collisions at 183 GeV*, Phys. Lett. **B453** (1999) 107.